AMTA 2008 PROCEEDINGS

Boston, Massachusetts
November 16-21, 2008

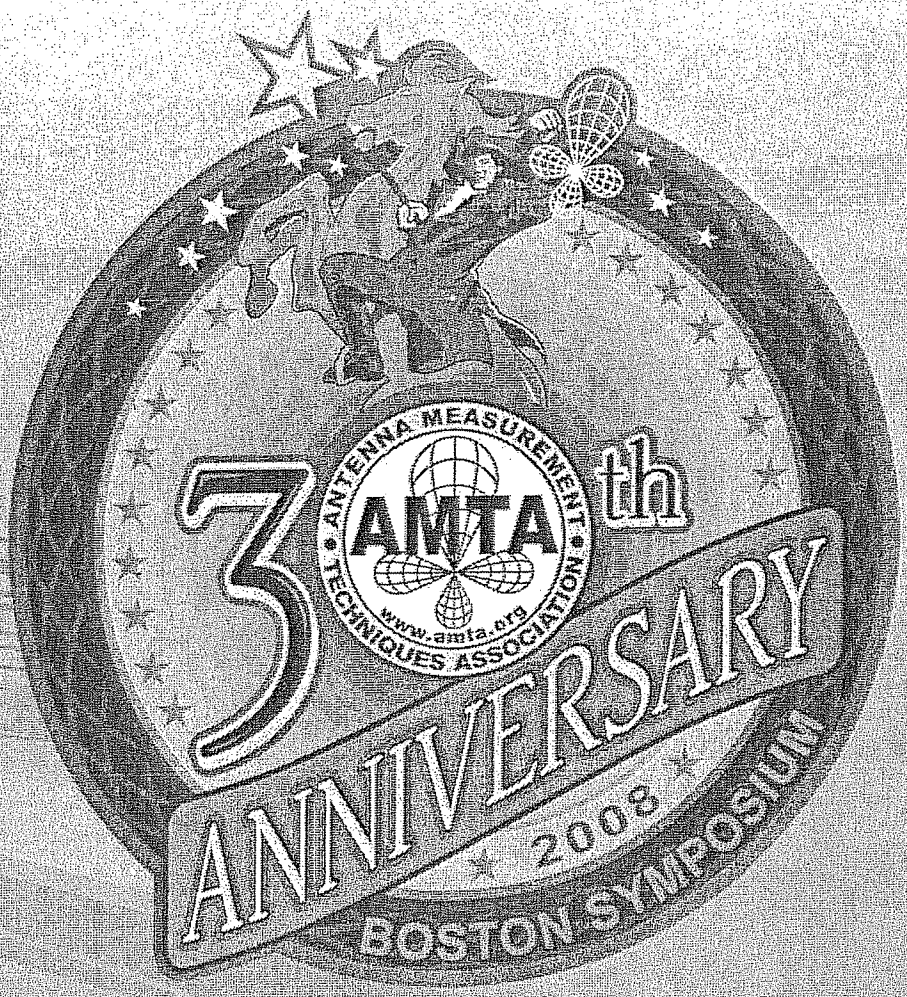

POLARIMETRIC CALIBRATION OF INDOOR AND OUTDOOR POLARIMETRIC RADAR CROSS SECTION SYSTEMS †

Lorant A. Muth

Electronics and Electrical Engineering Laboratory
National Institute of Standards and Technology
325 Broadway
Boulder, Colorado 80305-3328

ABSTRACT

We used a set of dihedrals to perform polarimetric calibrations on an indoor RCS measurement range. We obtain simultaneously *hh*, *hv*, *vh*, and *vv* polarimetric data as the calibration dihedrals rotate about the line-of-site to the radar. We applied Fourier analysis to the data to determine the polarimetric system parameters, which are expected to be very small. We also obtained polarimetric measurements on two cylinders to verify the accuracy of the system parameters. We developed simple criteria to assess the data consistency over the very large dynamic range demanded by the dihedrals. We examined data contamination by system drift, dynamic range nonlinearities, and the presence of background and noise. We propose improved measurement procedures to enhance consistency between the dihedral and cylinder measurements and to minimize the uncertainty in the polarimetric system parameters. The final recommended procedure can be used to calibrate polarimetrically both indoor and outdoor ranges.

Keywords: background, drift, measurement uncertainty, polarimetric calibration, radar cross section, reproducibility

1. Introduction

We use a set of dihedrals to perform polarimetric calibration on an indoor RCS measurement range. We measure polarimetric *hh*, *hv*, *vh*, and *vv* calibration data as the calibration dihedrals rotate about the line-of-site to the radar. The system parameters can then be obtained by use of Fourier analysis. The details of this theoretical procedure have been presented in [1,2]. The validity of the polarimetric system parameters can be verified by polarimetric measurements on cylinders, or other artifacts with known polarimetric scattering matrices [3].

Consistency between the polarimetric components of the data and between the dihedral and cylinder measurements needs to be established using simple consistency criteria (see Section 3, below).

Only when the data satisfy these simple consistency criteria can we have confidence that we can obtain polarimetric system parameters with small uncertainties. If data consistency cannot be established, a recalibration needs to be performed to improve the data.

Since we expect the polarimetric system parameters to be very small, accurate measurements (with low uncertainties) are essential. Known sources of RCS measurement errors, such as system drift, dynamic range nonlinearity, background and noise [4], and errors in the angle of rotation [5,6] must be minimzed to obtain system parameters with small uncertainties. Drift will most likely be a very important measurement error on outdoor ranges, and minimal in indoor ranges. The other sources of errors listed can be equally important on any RCS measurement range. Any set of polarimetric calibration data needs to be scrutinized with these sources of errors in mind. Procedures to correct for angular errors and system drift have been studied in [3,5,6]. These procedures can be applied to reduce measurement uncertainties.

The goal of this study is to develop and recommend a polarimetric calibration procedure in detail that can be used by both indoor and outdoor ranges.

Specifically, we will briefly address the following:

1. Review the theory of polarimetric calibration.
2. Present the polarimetric calibration data to review its essential features.
3. Present critera to evaluate polarimetric data consistency.
4. Derive the polarimetric system parameters with some estimate of uncertainty.
5. Consider further steps to be implemented to continue to explore and improve the calibration procedure.

† A U.S. governme[illegible] [illegible]ject to copyright in the United States

2. Theoretical Model

We use a rotating dihedral to calibrate a polarimetric radar. The receive matrix is given by

$$r = \begin{pmatrix} r_{hh} & r_{hv} \\ r_{vh} & r_{vv} \end{pmatrix}. \quad (1)$$

We assume reciprocity in the sense that the transmit matrix is $t = \tilde{r}$, the matrix transpose. After normalization, we can write

$$r = \begin{pmatrix} 1 & \epsilon_h \\ \epsilon_v & 1 \end{pmatrix}, \quad (2)$$

where

$$\epsilon_h = \frac{r_{hv}}{r_{hh}} \quad \text{and} \quad \epsilon_v = \frac{r_{vh}}{r_{vv}}. \quad (3)$$

The dihedral scattering matrix (in the high frequency limit) is given by

$$D(\theta) = k_D \begin{pmatrix} -\cos 2\theta & \sin 2\theta \\ \sin 2\theta & \cos 2\theta \end{pmatrix}, \quad (4)$$

where θ, with respect to the vertical, is the angle of rotation about the line-of-sight from the radar to the dihedral, and k_D depends on the dimensions of the dihedral and is assumed to be known. The polarimetric signal scattered from a dihedral is given by the matrix product

$$M(\theta) = krD(\theta)t. \quad (5)$$

Here, k is a complex constant. The matrix elements of M are

$$(kk_D)^{-1} M_{hh} = (-1 + \epsilon_h^2)\cos 2\theta + 2\epsilon_h \sin 2\theta, \quad (6)$$

$$(kk_D)^{-1} M_{vv} = (1 - \epsilon_v^2)\cos 2\theta + 2\epsilon_v \sin 2\theta, \quad (7)$$

$$(kk_D)^{-1} M_{hv} = (\epsilon_h - \epsilon_v)\cos 2\theta + (1 + \epsilon_h \epsilon_v)\sin 2\theta, \quad (8)$$

and

$$(kk_D)^{-1} M_{vh} = (\epsilon_h - \epsilon_v)\cos 2\theta + (1 + \epsilon_h \epsilon_v)\sin 2\theta. \quad (9)$$

For all polarizations, we can write

$$M_{pq} = c_{2,pq} \cos 2\theta + s_{2,pq} \sin 2\theta, \quad (10)$$

where p and q are either h or v. We can use Fourier analysis to obtain all coefficients $c_{2,pq}$ and $s_{2,pq}$ from the measured data.

The ratio of the measured $n = 2$ Fourier coefficients obtained from the data can be expressed in terms of the system parameters by use of the theoretical expressions for the coefficients in eqs (6 - 9). If the drift is not significant [3], we can solve for the polarimetric system parameters using the expressions

$$r_{2,h} = \frac{s_{2,hh}}{c_{2,hh}} = \frac{2\epsilon_h}{-1 + \epsilon_h^2} \quad (11)$$

and

$$r_{2,v} = \frac{s_{2,vv}}{c_{2,vv}} = \frac{2\epsilon_v}{1 - \epsilon_v^2}. \quad (12)$$

We note that these ratios are independent of all constants in eqs (6 - 9), and easily yield ϵ_q. In general,

$$\epsilon_q = \frac{I_q \pm \sqrt{1 + r_{2,q}^2}}{r_{2,q}}, \quad (13)$$

where $I_h = 1$ and $I_v = -1$. We obtain two parameters for each polarization that are negative reciprocals of each other. We always choose $\epsilon_q < 1$, which is true for RCS systems.

We can use a cylinder to verify the parameters. A cylinder's scattering matrix is given by

$$C_0 = \begin{pmatrix} C_{hh} & 0 \\ 0 & C_{vv} \end{pmatrix}. \quad (14)$$

Since a cylinder is nondepolarizing, the cross-polarization (off-diagonal) elements are 0. The polarimetric measurements on a cylinder are given by (see eq (5))

$$M_C = rC_0t. \quad (15)$$

The matrix components of M_C are either of first or second order in ϵ_q,

$$M_C = \begin{pmatrix} C_{hh} + \epsilon_h^2 C_{vv} & \epsilon_v C_{hh} + \epsilon_h C_{vv} \\ \epsilon_v C_{hh} + \epsilon_h C_{vv} & C_{vv} + \epsilon_v^2 C_{hh} \end{pmatrix}, \quad (16)$$

where the cross-polarimetric components are created only by the cross-polarization of the radar.

If we correctly specify ϵ_q, we can recover C_0 by using the inverses r^{-1} and t^{-1}, since

$$C_0 = r^{-1} M_C t^{-1}. \quad (17)$$

Uncertainties in ϵ_q will not allow us to recover the vanishing cross-polarimetric components in C_0 completely.

3. Polarimetric Calibration Data

We measured polarimetrically two 30.48×30.48 cm^2 and 15.24×15.24 cm^2 square dihedrals, and two cylinders with diameters 19.05 cm and 11.43 cm, and heights 8.89 cm and 5.33 cm, respectively. These are the widely used standard cylinders designated as '750' and '450' by the RCS measurement community. In Figure 1 we show the real and imaginary parts of the hh and the imaginary parts of the hv and vv measurements on the larger dihedral taken at 9.3 GHz. The copolar and cross-polar data were normalized to 1 at $\theta = 0°$ and $\theta = 45°$, respectively. Alignment of the dihedrals was checked by comparing the data at 0° and 180°.

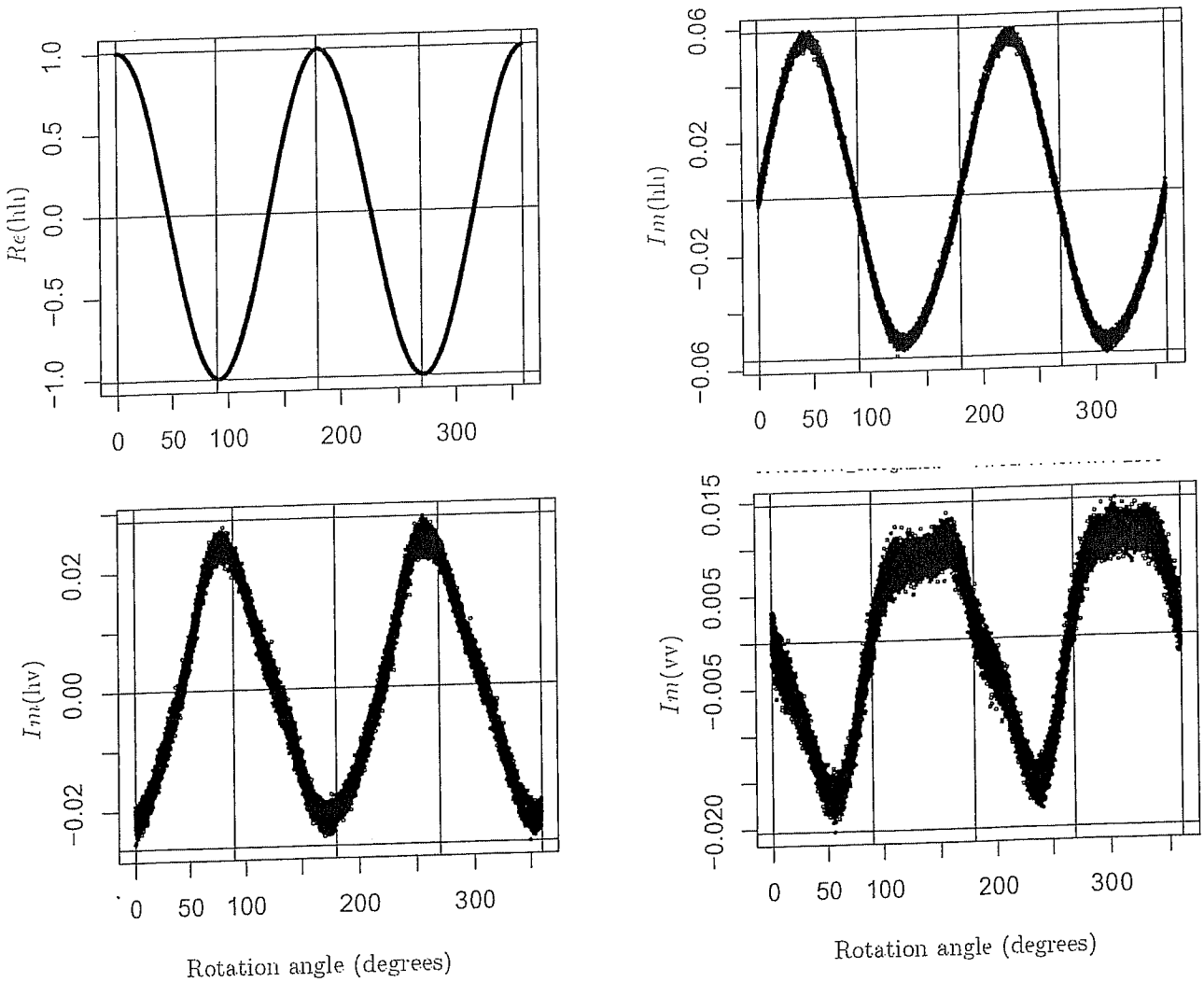

Figure 1. The real and imaginary parts of the hh and the imaginary parts of the hv and vv measurements made with the large dihedral. These are normalized data showing the relative amplitudes of the real and imaginary parts.

When we examine the uncalibrated polarimetric cylinder responses we see only data points scattered around a mean. Hence the plots (not shown) are not very revealing. We take the means to be the measured values. Drift in the data was not observed.

Altogether 18000 data points were collected for each artifact. The dihedrals were rotated 10 times, and each rotation lasted 3 minutes. The cylinders were stationary during the 30 minutes of data acquisition. The correct sinusoidal dependence of each polarimetric dihedral measurement is easily verified from eqs (6-9). Imaginary parts of the dihedral data are significantly noisier due to the low signal level at all angles. The actual dihedral response of each polarimetric component is given by eq (10), after the corresponding $c_{2,pq}$ and $s_{2,pq}$ cofficients have been determined by Fourier analysis. Because the dihedral is rotating and the background is stationary, the contribution of the background to the Fourier coefficients is greatly reduced, and the Fourier analysis significantly reduces the contribution of noise. Still, noise in the imaginary data will propagate an uncertainty into the imaginary parts of ϵ_q. The low level signals received from the cylinder are also noisy. The actual cylinder responses are taken to be the mean of the 18000 data points, thereby minimizing the effects of noise.

In Figure 2 we show the relative amplitudes (dB) of maxima and minima of the measurements on the dihedrals and cylinders. We include the corresponding theoretical values; one channel for each artifact is normalized to the measurements. The dynamic range of the data we intend to analyze exceeds 40 dB. We desire to determine and verify very small polarimetric system parameters using these data: obviously we are

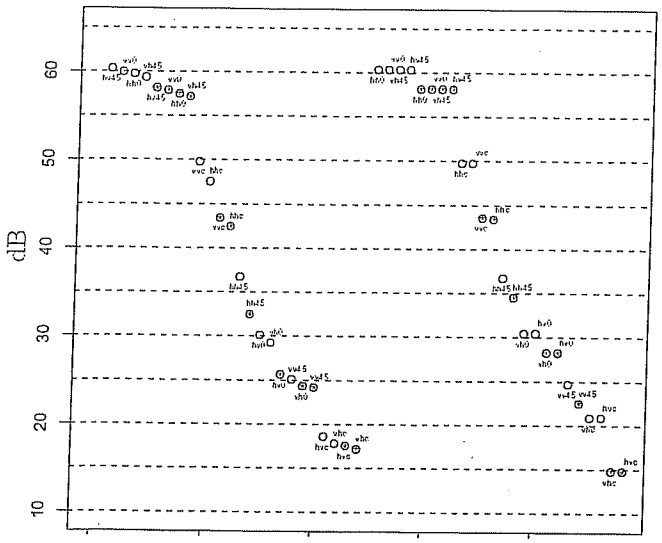

Figure 2. The sequence (x coordinate) of relative maxima and minima (dB) of uncalibrated dihedral and cylinder measurements and the normalized theoretical values. Labels indicate polarization and rotation angles, c is cylinders. * marks the smaller artifacts.

placing very stringent requirements of accuracy on the RCS measurement system. We can quickly come to some qualitative conclusion about the data. We can compare only relative amplitudes between theory and measurement, since the uncalibrated measurements reflect the channel amplifications, which are not necessarily the same. To obtain the theoretical values for the cylinders, we used the ϵ_q obtained with the large dihedral.

In Figure 2 we can spot immediately some data inconsistencies. For example, we examine the relative cross-polar measured and theoretical amplitudes for the cylinders. They are not in agreement, possibly indicating cross-polar contamination with some extraneous signal. This implies that we will not be able to verify that the system parameters obtained from the dihedral measurements will greatly reduce the cylinders' cross-polar response.

4. Polarimetric Consistency Criteria

In Figure 2, we saw an example of data set inconsistency; the relative cylinder measurements and the corresponding relative theoretical values do not agree.

In our complex data set we must demand consistency over a large dynamic range and also within the set of artifacts used to determine polarimetric system parameters. Only a consistent data set will produce system parameters with reasonable uncertainties.

We need to develop criteria (that are relatively easy to implement) to demonstrate data set consistency. Only then does it make sense to proceed to analyze the data to determine the system parameters. A very powerful diagnostic tool is the ratio of the measured cross-polar to copolar products [3],

$$\chi_m(\theta, \epsilon_{p,q}) = \frac{M_{hv} M_{vh}}{M_{hh} M_{vv}}. \tag{18}$$

$\chi_m(\theta, \epsilon_{p,q})$ is independent of channel-path amplifications and the properties of the dihedral; it depends only on the system parameters $\epsilon_{p,q}$. Once we determine $\epsilon_{p,q}$ (see Section 5 below), then we can form the ratio χ_r

$$\chi_r = \frac{\chi_m(\theta, \epsilon_{p,q})}{\chi_\epsilon(\theta, \epsilon_{p,q})} = 1, \tag{19}$$

where χ_ϵ is obtained from the right sides of eqs (6 - 9).

In Figure 3 we show χ_r for ten rotations for the large and small dihedrals, respectively. The rotations are delineated by vertical broken lines. The first rotation data of the large dihedral (top) seem to satisfy the requirement in eq (19) very well; there is an easily observable deviation from 0 dB as the measurement sequence continues beyond the first rotation. For the small dihedral (bottom) we observe that the last three rotations best satisfy eq (19). Thus, the first rotation of the large dihedral and the last three rotations of the small dihedral provide consistent data sets. We observe phase variations in χ_r around 0 in both cases. This is not surprising, since we are comparing unfiltered to filtered data. We expect the phase deviations to decrease after the data has been filtered by use of Fourier analysis to eliminate noise, background and any stationary extraneous signals that might be present.

A similar analysis can be performed by use of the cylinder data. We will not do this here due to space limitations, but will present the results at the conference. We note that eq (18) can be also used to monitor drift by evaluating the numerator and denominator at different points in the measurement sequence.

There are additional criteria that can be used to quickly evaluate data integrity. Theoretically, the hv and vh responses are equal for the dihedrals and cylin-

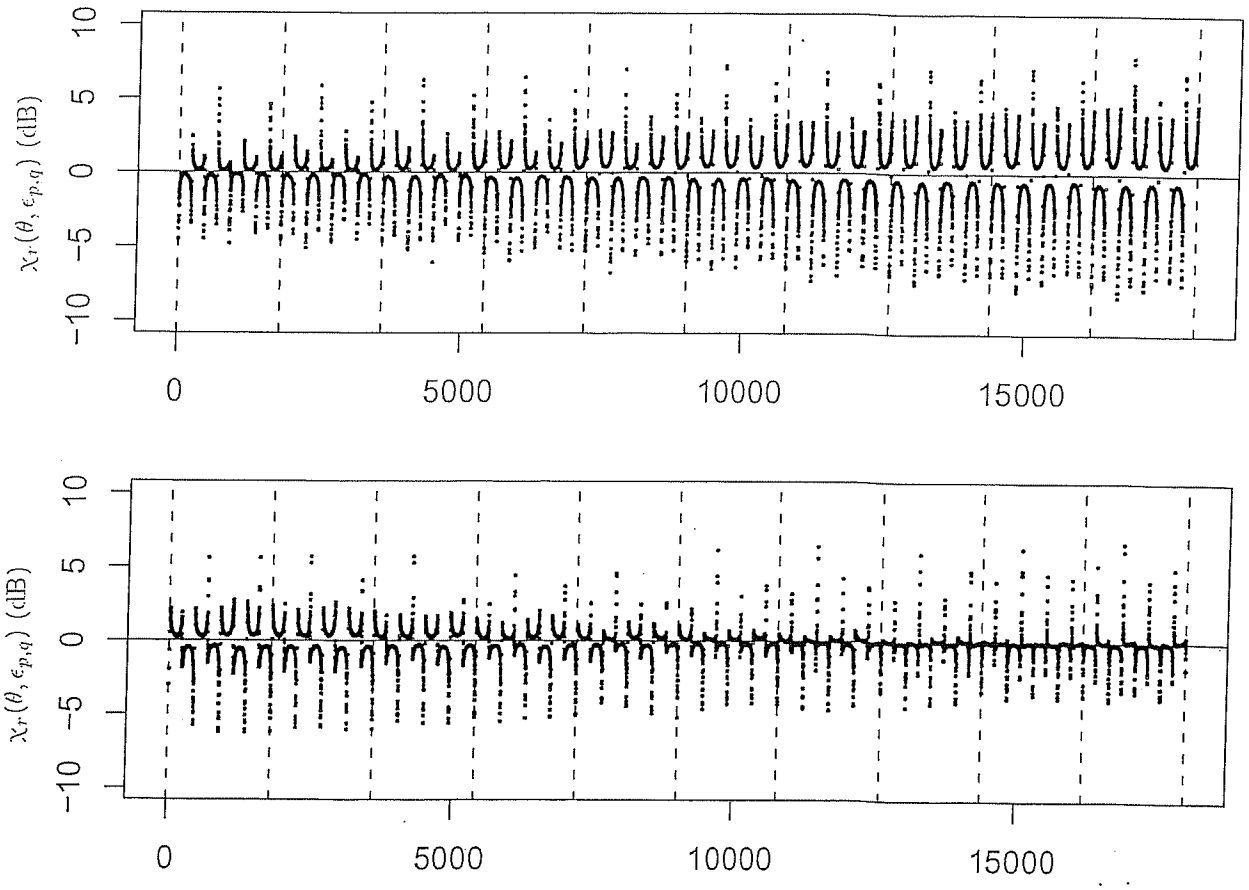

Dihedral data sequence for 10 rotations

Figure 3. $\chi_r(\theta, \epsilon_q)$ amplitudes (dB) for the large (top) and small dihedrals for 10 rotations.

ders, as seen in eqs (8), (9)) and (16). The radar measurement system was configured so that the cross-polar channel amplifications are not equal. In practice this is usually the case. It follows that throughout the measurement sequence, the ratio of the hv to vh measurements should be a constant equal to the ratio

$$\frac{M_{hv}}{M_{vh}} = \frac{R_{hv}}{R_{vh}}, \tag{20}$$

where R_{pq} are the constant channel-path amplifications. These ratios evaluated for the dihedrals and the cylinders should agree. Contamination by drift, noise and target-background interactions can be easily monitored this way.

We can also check the copolar ratios. For the dihedrals,

$$\frac{M_{hh}}{M_{vv}} = -\frac{R_{hh}}{R_{vv}} + O(\epsilon_q^2), \tag{21}$$

and for the cylinders,

$$\frac{M_{hh}}{M_{vv}} = \frac{R_{hh}}{R_{vv}} \frac{C_{hh}}{C_{vv}} + O(\epsilon_q^2). \tag{22}$$

The cylinder's copolar ratio can be computed from the matrix elements in eq (16), where we must use the $\epsilon_{p,q}$ obtained with the dihedrals. Ideally the copolar channel-path amplification ratios in eqs (21-22) are equal. Hence, the consistency between the dihedral and cylinder measurements can be monitored. Data with significant problems will not reproduce the theoretical ratio in eq (22). We will show more detailed results using eqs (20 - 22) at the conference.

5. Polarimetric Data Analysis

We analyze each polarimetric measurement made on the large dihedral to obtain the $n = 2$ Fourier coefficients, as required by eq (10). We then equate the ratios of these coefficients to their theoretical ratios, as in eqs (11) and (12), and obtain $\epsilon_{p,q}$ using eq (13).

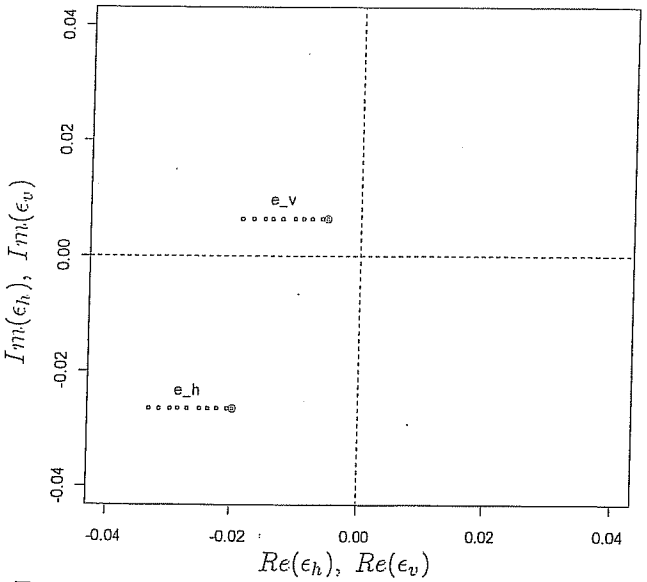

Figure 4. The polarimetric system parameters $\epsilon_{p,q}$ obtained in 10 rotations with the large dihedral.

In Figure 4 we plot the $\epsilon_{p,q}$ for 10 rotations. The initial rotation is identified with double circles. We observe a change in one direction on the real axis as a function of rotation. This is similar to the deviations from 0 dB seen in Figure 4. This could be due to a positive accumulation of angular errors. We can show from eq (6) that at 45°,

$$\delta M_{qq} = \pm 2(1 - \epsilon_q^2)\delta\theta \tag{23}$$

which is essentially real. Since the $M_{qq}(45°) = 2\epsilon_q$, an error in the real part of the measurement will linearly propagate into $Re(\epsilon_q)$. Further data analysis is needed to establish this interpretation. For each pair of $\epsilon_{p,q}$ we can use eq (17) to verify that the cross-polar cylinder measurements can be substantially reduced.

We saw in Figure 2 that the cylinder's cross-polar response may be contaminated. We tried to reduce the cylinder's cross-polarization matrix elements, but we obtained a reduction by only a few dBs. We do not expect that contaminated cross-polar data will be inverted using eq (17). Consider a simple model to illustrate: (1) assume error-free copolar calibrations and $\epsilon_{p,q}$, and assume that the cross-polar channels are calibrated with $\Gamma' = \Gamma_0 + \delta\gamma$, where Γ_0 is error-free and $\delta\gamma$ is the error in the calibration constant. Then, eqs (15-17) show that the cross-polar ratios of the inverted calibrated cylinder matrix will not vanish, but will be

$$\frac{\delta\gamma}{\Gamma'}\frac{M_{C,pq}}{M_{C,pp}} + O(\epsilon). \tag{24}$$

For large $\delta\gamma$, at low signal levels, the inversion in eq (17) will completely fail.

6. Future Efforts

Currently, the *small system parameters* $\epsilon_{p,q}$ we seek can be determined only with large uncertainties. *This problem needs to be addressed explicitly to reduce these uncertainties.* We plan to develop further consistency tests to verify polarimetric data integrity. We plan to make measurements on larger cylinders to increase the cross-polar signals to reduce noise and the influence of low-level extraneous signals. We will explore ways to correct data that are known to be inconsistent, and explore the implications of eq (19) in depth. Our final objective is to recommend a set of calibration procedures to calibrate polarimetric indoor and outdoor measurement ranges *repeatably and with small uncertainties.*

Acknowledgement

The contributions by Dr. Dean Mensa, Ken Vecchio, Dave Loucks, Tai Kim and Dr. Ken Oh at the Radar Reflectivity Laboratory, NAWCWD, Point Mugu, CA and support by the DoD Coordinated Calibration Group are greatfully acknowledged.

References

[1] L. A. Muth, R. C. Wittman and R. L. Lewis, "Polarimetric calibration of reciprocal antenna radars," *Antenna Measurement Techniques Assoc. (AMTA) 1995 Proceedings*, 1995.

[2] M. W. Whitt and F. T. Ulaby, "A polarimetric radar calibration technique with insensitivity to target orientation," *Radio Science*, vol. 25, pp. 1137 – 1143, 1990.

[3] L. A. Muth, "Cross-polarization parameters in the presence of drift in radar cross section measurements," *Antenna Measurement Techniques Assoc. (AMTA) 2006 Proceedings*, 2006.

[4] Wittmann, R.C., Francis, M.H., Muth, L.A., Lewis, R.L., "Proposed uncertainty analysis for RCS measurements," Natl. Inst. Stand. Technol. NISTIR 5019, January 1994

[5] L. A. Muth, C. William, D. Morales, and T. Conn, "Angular errors in polarimetric radar cross section calibration using a rotating dihedral," *Antenna Measurement Techniques Assoc. (AMTA) 2005 Proceedings*, 2005.

[6] L. A. Muth, C. Johnson, D. Morales and T. Conn, "Angular errors in polarimetric radar cross section calibration using a rotating dihedral," *NIST Technical Note 1539*, National Institute of Standards and Technology, U.S. Department of Commerce, 2005.